

The effect of cloudiness on new-particle formation: investigation of radiation levels

Elham Baranizadeh¹⁾, Antti Arola²⁾, Amar Hamed^{1)†}, Tuomo Nieminen³⁾⁴⁾, Santtu Mikkonen¹⁾, Annele Virtanen¹⁾, Markku Kulmala⁴⁾, Kari Lehtinen²⁾ and Ari Laaksonen¹⁾⁵⁾

¹⁾ Department of Applied Physics, University of Eastern Finland, P.O. Box 1627, FI-70211 Kuopio, Finland

²⁾ Finnish Meteorological Institute, P.O. Box 1627, FI-70211 Kuopio, Finland

³⁾ Helsinki Institute of Physics, P.O. Box 64, FI-00014 University of Helsinki, Finland

⁴⁾ Department of Physics, P.O. Box 64, FI-00014 University of Helsinki, Finland

⁵⁾ Finnish Meteorological Institute, Research and Development, P.O. Box 503, FI-00101 Helsinki, Finland

Received 13 Jan. 2014, final version received 15 Apr. 2014, accepted 16 Apr. 2014

Baranizadeh E., Arola, A., Hamed, A., Nieminen, T., Mikkonen, S., Virtanen, A., Kulmala, M., Lehtinen, K. & Laaksonen, A. 2014: The effect of cloudiness on new-particle formation: investigation of radiation levels. *Boreal Env. Res.* 19 (suppl. B): 343–354.

The effect of cloudiness on the occurrence of atmospheric new-particle formation events at two measurement stations, SMEAR II in Hyytiälä, Finland and San Pietro Capofiume (SPC) in Italy, was investigated. As an indicator of cloudiness, we use the relative radiation intensity (I/I_{\max}) defined as the ratio of measured global radiation and the modeled clear-sky global radiation. We studied the relationship between the occurrence of new-particle formation (NPF) events and I/I_{\max} using multi-year data sets. The results showed that, at both sites, the radiation intensity (I) should be at least about 50% of its maximum possible value (I_{\max}) for a clear NPF event to occur. In SPC, clearly higher relative radiation intensity was typically required for the occurrence of an NPF event than in Hyytiälä. Also, the features of anomalous days, i.e. either NPF events that occurred in cloudy conditions or non-events that occurred in clear-sky conditions, were explained using the environmental variables sulfur dioxide and condensation sink.

Introduction

Atmospheric new-particle formation (NPF) events, i.e. nucleation and the subsequent growth of the newly formed particles have been well documented in many different environments all around the world (Kulmala *et al.* 2004a and references therein). Many studies have been conducted to find out the important variables causing and preventing the NPF events. Sulfur

dioxide (SO₂) (together with OH radicals) is an important precursor to NPF as its oxidation produces sulphuric acid (H₂SO₄) which is a crucial component to initiate both the nucleation event and subsequent growth of nucleated clusters to 3 nm which is the detection limit of traditional DMPS systems which are still used in most long-term NPF measurements (Weber *et al.* 1996, Kulmala *et al.* 2004, 2006, Sihto *et al.* 2006, Kulmala and Kerminen 2008, Laak-

sonen *et al.* 2008, Kerminen *et al.* 2010, Kuang *et al.* 2010, 2012, Sipilä *et al.* 2010, Metzger *et al.* 2010, Mikkonen *et al.* 2011). Hyvönen *et al.* (2005) showed that low relative humidity (RH) and condensation sink are related to the occurrence of NPF events in Hyytiälä (Finland). The ambient pre-existing particles suppress NPF either by being a condensation surface for low-volatility vapors or by scavenging small clusters formed by nucleation. Both of these sinks tend to slow down — or in extreme cases inhibit — the growth of particles to detectable sizes. Therefore, low condensation sink values increase the probability of detectable NPF events. Moreover, RH, which is related to cloudiness, tend to correlate negatively (in particular at $RH > 60\%$) with the intensity of solar radiation via the attenuation of radiation reaching the boundary layer, resulting in a reduction of the OH concentration (which is strongly correlated with solar radiation, in particular the UV component) and thereby also the production of sulphuric acid (Hamed *et al.* 2011). Thus, high values of RH do not favour the occurrence of an NPF event.

The importance of solar radiation as a driver for new-particle formation has been confirmed in the literature. Pirjola (1999) applied a sectional model (AEROFOR) to find out the impact of UV-B radiation on the formation of new particles by a binary nucleation mechanism of H_2SO_4 – H_2O . She investigated the combined effect of increasing both UV-B levels and concentrations of biogenic volatile organic compounds (BVOC), and found that when the increase of the BVOC (e.g. by 40%) concentration dominated over the increase of the of UV-B radiation intensity (e.g. by 30%), the number concentration of freshly-formed particles decreased, and vice versa. In the base case with BVOC emission remaining unchanged, the increased UV-B radiation intensity increased the number concentration of freshly-formed particles linearly, so that e.g. the number concentration of particles became 2.5 fold with a 50% increase in the UV-B radiation.

Boy and Kulmala (2002) suggested that a low atmospheric water-vapor content, low condensation sink and high solar radiation intensity, in particular the UV-A component, create favorable circumstances for NPF. Moreover, they concluded that the radiation level required for the appearance

of the smallest detectable 3 nm particles is more than one third of the daily maximum radiation and that nucleation stops when the radiation decreases below this value. Sogacheva *et al.* (2008) showed that the seasonality and inter-annual differences in the event frequency can be explained by the seasonal and yearly differences, respectively, in the distribution of days with the low cloud amount. They also concluded that cloudiness of less than 5 octas (half or less of the sky is covered by clouds) is one of the necessary conditions for an NPF event to occur. Moreover, they suggested that cloudiness of more than 4 octas is a key parameter for turning an NPF event to a less quantifiable event (called class Ib or II event based on Dal Maso *et al.* 2005) and prevents the occurrence of clear and well-quantifiable events (called class Ia event). However, providing both the type and the amount of clouds from satellite and/or ground-based observations is a challenging issue which often is subject to error (Schiffer and Rossow 1983). For example low radiance reaching the satellite sensor from the snow-covered land leads to inaccurate estimates of cloud coverage.

In this study, we concentrate on the efficiency of clouds to attenuate solar radiation — not the observable amount or type of clouds — which in turn affects the occurrence of NPF events. Here, in addition to the level of absolute radiation, we used a relative radiation intensity as an indicator of the presence of clouds. This allowed us to follow changes in the aerosol size distribution and other environmental variables (e.g. RH, condensation sink, concentration of SO_2 or ozone) when clouds were present.

Data and methods

The research was carried out at two stations: (1) SMEAR II characterized by boreal coniferous forest, located in Hyytiälä ($61^{\circ}51'N$, $24^{\circ}17'E$, 181 a.s.l.), southern Finland, and (2) San Pietro Capofiume (SPC) measurement station ($44^{\circ}39'N$, $11^{\circ}37'E$) located NE from the city of Bologna, Po Valley, Italy. The main pollution sources affecting the Hyytiälä station are the city of Tampere (60 km away) and also the station buildings close (0.5 km) to the measurement instruments. These effects are mostly seen when

the wind is in the southwest direction (Kulmala *et al.* 2001, Boy and Kulmala 2002). Po Valley is a high-population area and the largest industrial, trading and agricultural area in Italy (*see* Hamed *et al.* 2007 for further information about the site). The particle size distribution measurements were carried out using the Differential Mobility Particle Sizer (DMPS) systems in the diameter size ranges of 3–500 nm and 3–600 nm in Hyytiälä and SPC, respectively.

We calculated a relative radiation intensity parameter (hereafter III_{\max}) as an indicator of cloudiness, defined as the ratio of measured global radiation I (W m^{-2}) at a given time divided by the modeled clear-sky global radiation I_{\max} (W m^{-2}). Therefore, III_{\max} indicates what fraction of the radiation intensity corresponding to clear-sky conditions reached the ground after the attenuation caused by clouds.

We analyzed III_{\max} between the NPF start and end times (i.e. the times when the 3-nm particle production starts and ends, respectively; hereafter NPF-time-window) for the NPF event days, and from one hour after sunrise until noon for the days with no NPF and for the undefined days. The NPF-time-window was defined visually from the contour plots of the evolution of the number size distribution (Fig. 1).

The global radiation intensity (I) was measured at the SMEAR II station in the time resolution of 30 min during 2002–2012. The radiation data collected from the SPC station were hourly averaged for the period March 2002–April 2005 (the data used in Hamed *et al.* 2007). For both sites, the I_{\max} data were downloaded from the AERONET website (<http://aeronet.gsfc.nasa.gov/>) and were based on modeling at clear-sky conditions. Note that these data were not available for the exact location of the SPC station; instead we used the closest possible station from the database, Modena ($44^{\circ}39'N$, $10^{\circ}56'E$), located on the south side of the Po Valley. As aerosol and cloud effects are not present in the modeled I_{\max} data, this approximation is reasonable. The I_{\max} data of SPC were converted into hourly averages to be consistent with the time resolution of actual global radiation data.

We classified the NPF event days as “quantifiable” (Q) or “non-quantifiable” (NQ) according to the criteria introduced by Dal Maso *et al.*

(2005) based on whether or not the event was homogeneous enough to make it possible to quantify its basic characteristics, such as the particle formation and growth rates. We left out the days when the DMPS was broken, i.e. days when the aerosol size distribution data were either completely missing or corrupted. Therefore, our data pool consisted of event (E), non-event (NE) and undefined days, the last ones being the days during which the evolution of the size distribution was too unclear for a definitive determination of whether or not NPF had been occurring. Due to missing measured radiation data, especially from the SPC station, the III_{\max} data could not be evaluated for all days.

Results and discussion

The number of the event, non-event and undefined days, for which the III_{\max} data were available, was determined for each season for later analysis (Fig. 2). In 2003, the measured radiation levels during most event days were higher than during non-event days at both sites (Fig. 3). Still, the radiation intensity I was clearly not a good enough predictor of whether a nucleation event occurred or not. At both sites, there were several non-event days in the summer when the daily-mean radiation intensity I was higher than on the event days occurring during the other seasons. Our hypothesis was that a clear day e.g. in spring is a more likely candidate for an event day than a cloudy day in summer, even if radiation on the summer day is of higher intensity than that on the spring day, and that such a feature can be explained by studying the relative radiation intensities, III_{\max} , instead of the absolute values of the radiation intensity. In addition to event occurrence, we also considered the strength NPF events by looking at particle formation and growth rates (*see* Dal Maso *et al.* 2005) as functions of I and III_{\max} (Fig. 4). Neither the formation nor growth rate seemed to be related to I , except that the highest growth rates occurred mostly at $I > 550 \text{ W m}^{-2}$. The situation was quite different for III_{\max} : the particle formation rates $> 2 \text{ cm}^{-1} \text{ s}^{-1}$ were limited to the values of III_{\max} larger than about 0.7, and particle growth rates larger than about 5 nm h^{-1} were mostly limited to

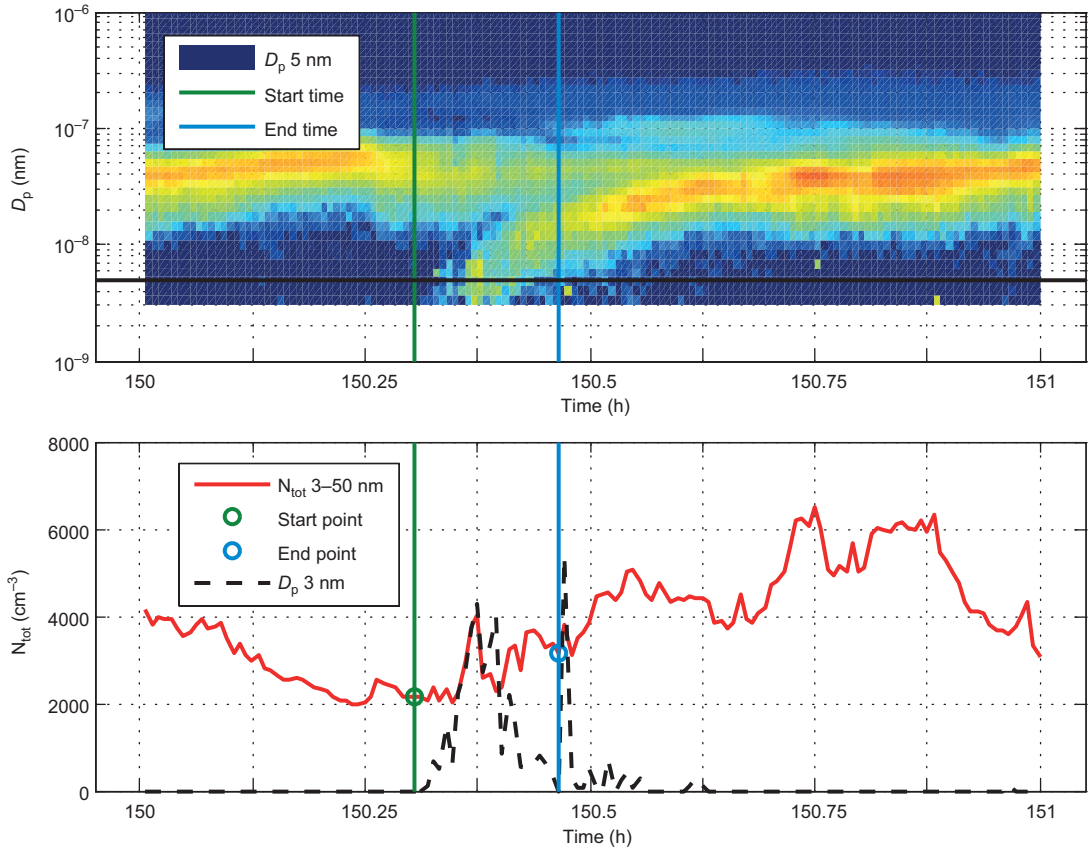


Fig. 1. New-particle formation event on 29 May 2012 in Hyttiälä, Finland. The time interval the between green and blue vertical lines shows the period of appearance of 3 nm particles. On this day, the detection limit of the DMPS system was 3 nm.

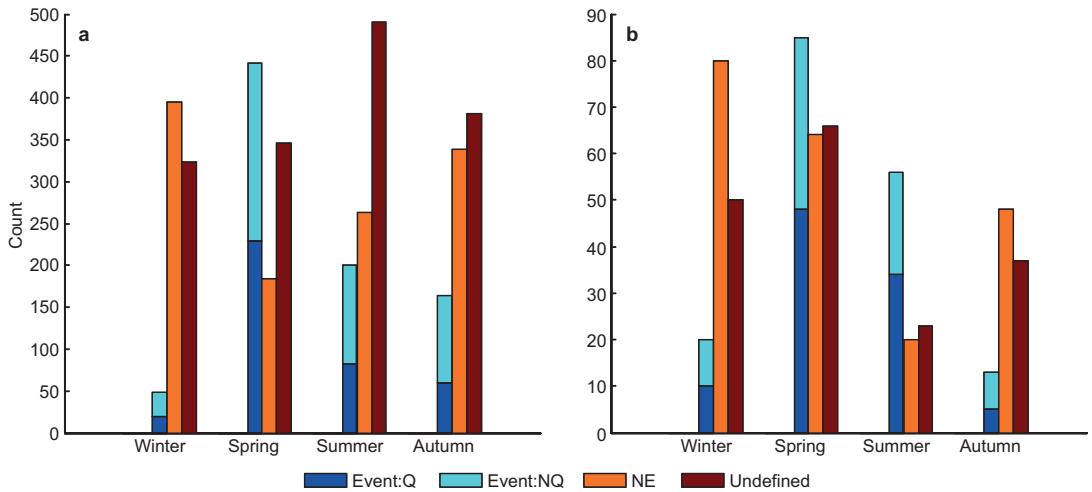


Fig. 2. The number of quantifiable (Event:Q) and non-quantifiable (Event:NQ) events, non-events (NE) and undefined days in winter (Dec., Jan., Feb.), spring (Mar., Apr., May), summer (Jun., Jul., Aug.) and autumn (Sep., Oct., Nov.) in (a) Hyttiälä during 2002–2012 and (b) SPC during March 2002–April 2005.

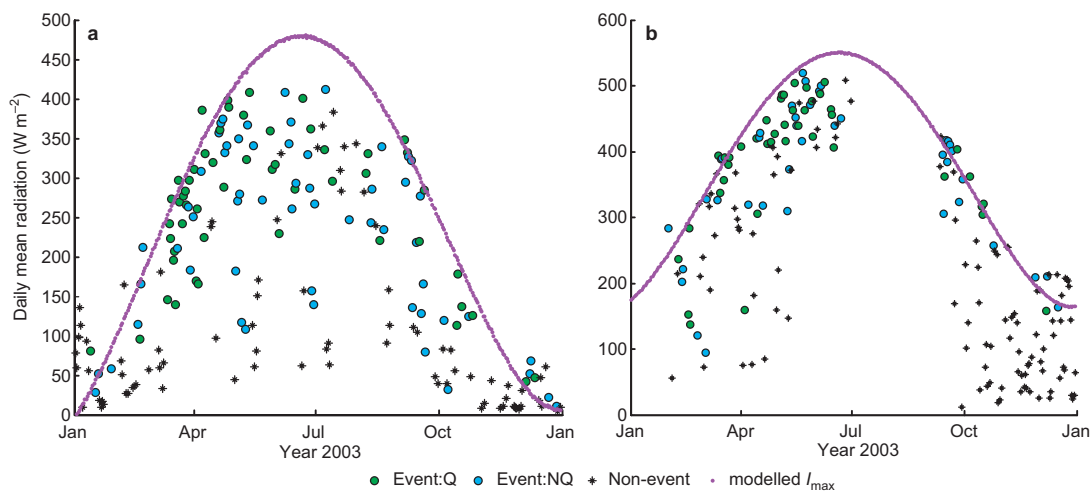


Fig. 3. Daily-mean global radiation in 2003 in (a) Hyytiälä and (b) San Pietro Capofiume. Event:Q = quantifiable days, Event:NQ = non-quantifiable days. The magenta curves show the modeled daily-mean clear-sky radiation intensity (I_{\max} ; W m^{-2}). The wintertime data points above the magenta curves were most likely caused by measurement or modeling errors related to the short daytime duration and low values of the absolute radiation intensity. In the data analysis, III_{\max} values larger than one were left out.

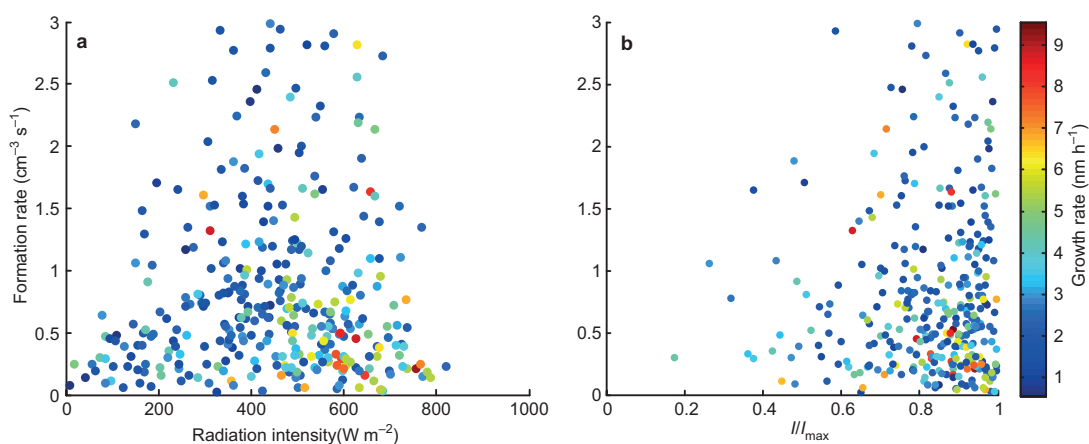


Fig. 4. The formation rates of 3–25 nm particles against (a) global radiation intensity, and (b) III_{\max} . Both global radiation intensity and III_{\max} were averaged over the time window of NPF on each event day. The data are from Hyytiälä in 1996–2011. The color map indicates the growth rates of 3–25 nm particles.

clear-sky conditions with the average value of $II_{\max} > 0.8$

Analysis of NPF event occurrence

Overall behavior

The values of III_{\max} were averaged over the time window of NPF for each event day and over the time window when no NPF was taking place for

the non-event and undefined days. We defined 20 average ranges for III_{\max} with a spacing of 0.05 and calculated the fraction of event days (Δ_E) and non-event days (Δ_{NE}) for each given III_{\max} range (Fig. 5). The results showed clearly that, typically high values of Δ_E corresponded to high values of III_{\max} and high values of Δ_{NE} corresponded to low values of III_{\max} . At both sites, the radiation intensity, I , had to be at least 50% of its maximum possible value, I_{\max} , for a quantifiable NPF event to occur. In Hyytiälä, the occurrence

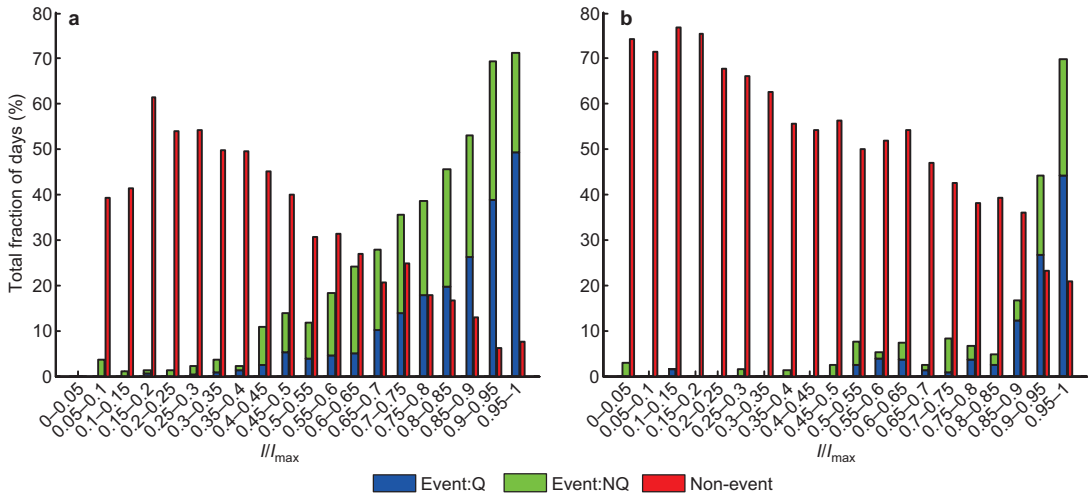


Fig. 5. Total fractions (%) of quantifiable event (Event:Q), non-quantifiable event (Event: NQ) and non-event days for the different value ranges of III_{\max} (a) during 2002–2012 in Hyttiälä, and (b) during March 2002–April 2005 in SPC. Note that the values of III_{\max} were averaged over the time windows of NPF events or non-events.

of an NPF event in partly-cloudy conditions was more likely than in SPC where almost clear-sky conditions were required (but did not a guarantee) for an NPF event to occur.

Seasonal behavior

To investigate the seasonal differences in the effect of cloudiness on the occurrence of NPF, a similar analysis as above (Fig. 5) was made separately for the four seasons in Hyttiälä (Fig. 6). The data were too scarce for such an analysis for SPC. Clear-sky conditions (e.g. $III_{\max} > 0.8$) guaranteed an NPF event with a very high probability during spring (Fig. 6b), and less so during other seasons. A rather clear separation between the events and non-event days was also visible in autumn (Fig. 6d), with the majority of the events taking place at $III_{\max} > 0.4$. In summer, the percentage of event days increased with an increasing value of III_{\max} , yet also non-events were possible over the whole range of values of III_{\max} (Fig. 6c). In winter, the event probability was low under all conditions, even though most events occurred at high values of III_{\max} (Fig. 6a). In all seasons, there were a few NPF event days at low values of III_{\max} (e.g. in the range 0.05–0.2: 22 Feb. 2008, 20 Apr. 2012, 21 Jul. 2011, 9 Sep.

2010), but these were mostly weak events. In addition, there were several NE days at high values of III_{\max} , especially during winter. We investigated the causes for these anomalous days by looking into the possible effects of other variables (*see below*). Another noteworthy outcome was that while previous studies found a summer minimum and secondary autumn maximum in the NPF event frequency in Hyttiälä (Dal Maso *et al.* 2005, Kulmala *et al.* 2004), no such behavior was observed in this study (Fig. 2).

Start and end times of NPF events

We studied the values of III_{\max} at the start and end of the NPF events in order to better understand the radiation level required to start and stop an event (Fig. 7). In SPC, only 17% of the events started at $III_{\max} < 0.8$ (Fig. 7b), whereas in Hyttiälä the corresponding fraction was 35% (Fig. 7a). Starting an event under (partially) cloudy conditions was more probable in Hyttiälä than in SPC. Interestingly, the distribution of event frequency did not depend much on whether the value of III_{\max} was calculated at the start (Fig. 7a and b) or end (Fig. 7c and d) of NPF. This shows that, in most cases, the events did not stop because of an increased cloudiness.

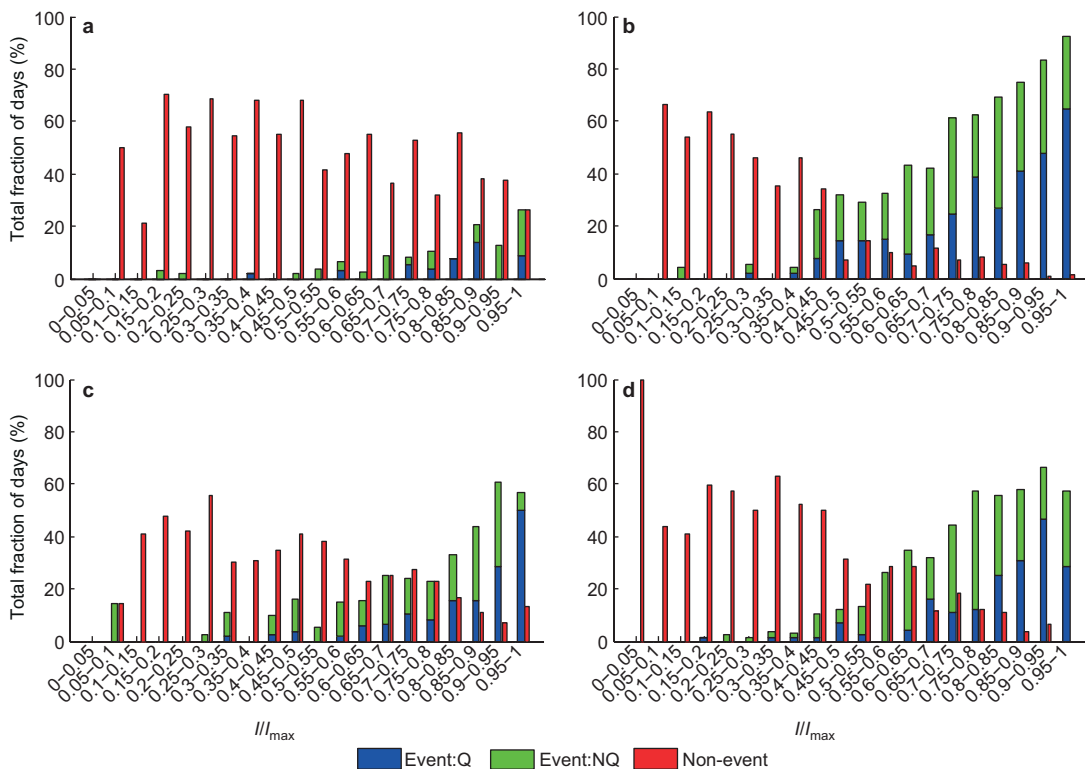


Fig. 6. Total fractions (%) of quantifiable event (Event:Q), non-quantifiable event (Event: NQ) and non-event days for the different value ranges of $///I_{max}$ in (a) winter, (b) spring, (c) summer and (d) autumn in Hyytiälä during 2002–2012.

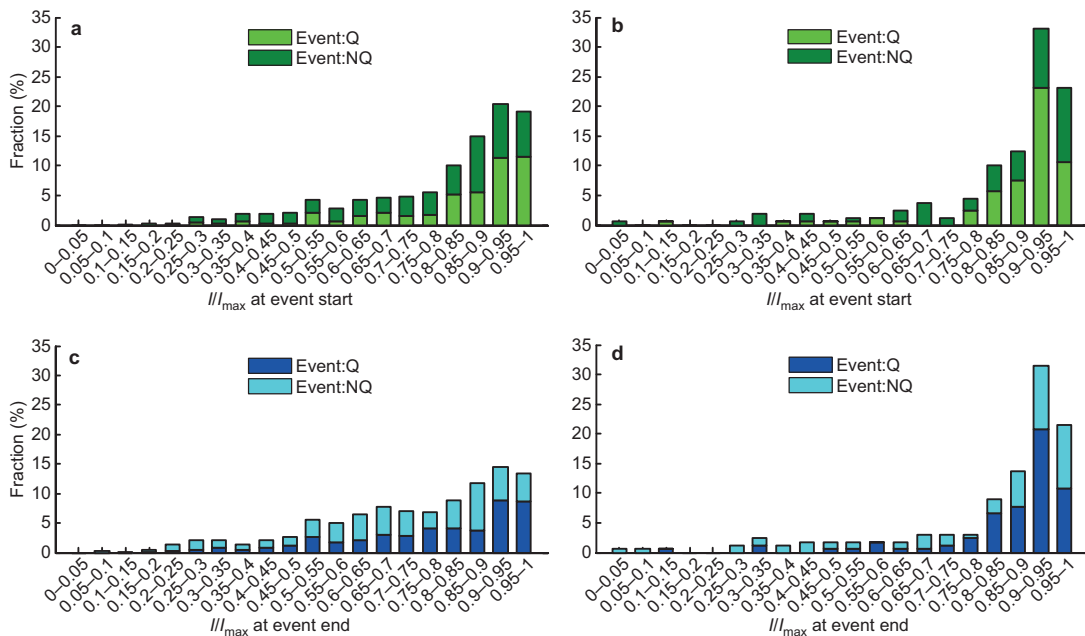


Fig. 7. Fraction of quantifiable (Event:Q) and non-quantifiable (Event:NQ) events as a function of $///I_{max}$ when the value of $///I_{max}$ was calculated at the start (panels a and b) or end (panels c and d) of NPF during the period 2002–2012 in Hyytiälä (panels a and c) and during March 2002–April 2005 SPC (panels b and d).

Investigations of anomalous days

Events associated with low III_{\max} values

The NPF event days having cloudy skies during the whole or a substantial part (at least one hour) of the time window of NPF were considered anomalous days, as were also the non-event days that had clear-sky conditions for a substantial part of the time when no NPF was taking place. The hours with $III_{\max} < 0.5$ and $III_{\max} > 0.8$ were chosen as cloudy and clear-sky hours, respectively. We found 70 and 16 NPF event days in Hyttiälä and SPC, respectively, with $III_{\max} < 0.5$ for more than an hour (Table 1).

We considered several quantities, including RH (%), condensation sink (CS), and concentrations of SO₂ (ppb), O₃ (ppb), NO₂ (ppb) and H₂O (ppth), in order to get insight into the atmospheric conditions that could favor NPF during cloudy days. We extracted the diurnal behaviour of these quantities (for example days *see* Fig. 8) and made scatter plots between the environmental data and CS (Figs. 9 and 10). We made a separation between cloudy hours for anomalous NPF event days, clear-sky hours for anomalous non-event days, clear-sky hours for normal NPF event days and cloudy hours for normal non-event days (Tables 2 and 3).

There was an inverse relation between the values of III_{\max} and RH at both sites. The scatter plots between RH and CS for normal event and non-event days (Figs. 9e and 10d) showed a clear division between the event ($III_{\max} > 0.8$) and non-event (and $III_{\max} < 0.2$) days, so that above RH of about 75% only few events occurred. On anomalous days, CS affected the division between the event and non-events days (Figs. 9b

and 10b). Put together, NPF events were highly likely at high values of III_{\max} , and therefore at relatively low RH, as long as the value of CS was not too high. In terms of the H₂O concentration, the anomalous event days were at least to some extent separated from the anomalous non-event days (Fig. 9c), whereas the normal events and non-events were not (Fig. 9f).

The anomalous NPF event days could be categorized into three types as follows:

Type 1: NPF started in cloudy conditions, but clouds disappeared during the event. For this event type to occur in Hyttiälä, the SO₂ concentration level of about twice that on normal NPF event days was required (Table 1). In addition, CS values were on average lower than during normal event days. The NPF event on 8 Apr. 2003 is an example of this type (Fig. 8a): clouds appeared at the start of the event and lasted for about two hours, after which the sky cleared for the rest of NPF. In SPC, low values of CS (average being about half of the normal event value) were associated with the type 1 events.

Type 2: Clouds appeared at some time during NPF. However, the event continued after the sky cleared again. At both sites, this event type was characterized by very low values of CS, which apparently compensated for the low concentration levels of SO₂. The event on 4 Oct. 2002 in Hyttiälä (Fig. 8b) is an example of this type.

Type 3: Clouds were present during almost whole NPF (e.g. 6 Oct. 2002; Fig. 8c). The average values of SO₂ and CS did not differ very much from those during normal NPF events. Type 3 events were very weak.

Almost all anomalous NPF events were non-quantifiable with low concentrations of ultrafine particles in both sites. The main quantities that favored the events, besides cloudiness, were relatively low values of CS and similar SO₂ concentration levels as observed on normal NPF event days. At the same time, high RH (average value 72%) and high H₂O concentrations (average value 8 ppb) were measured.

Table 1. The number of NPF events with $III_{\max} < 0.5$ (i.e. cloudy condition) at the start of the event (Type 1), during a shorter period between the event start and end (Type 2), during whole period of NPF (Type 3), and at the end of the event (interrupted events).

	Type 1	Type 2	Type 3	Interrupted events
Hyttiälä	18	28	24	56
SPC	7	3	6	10

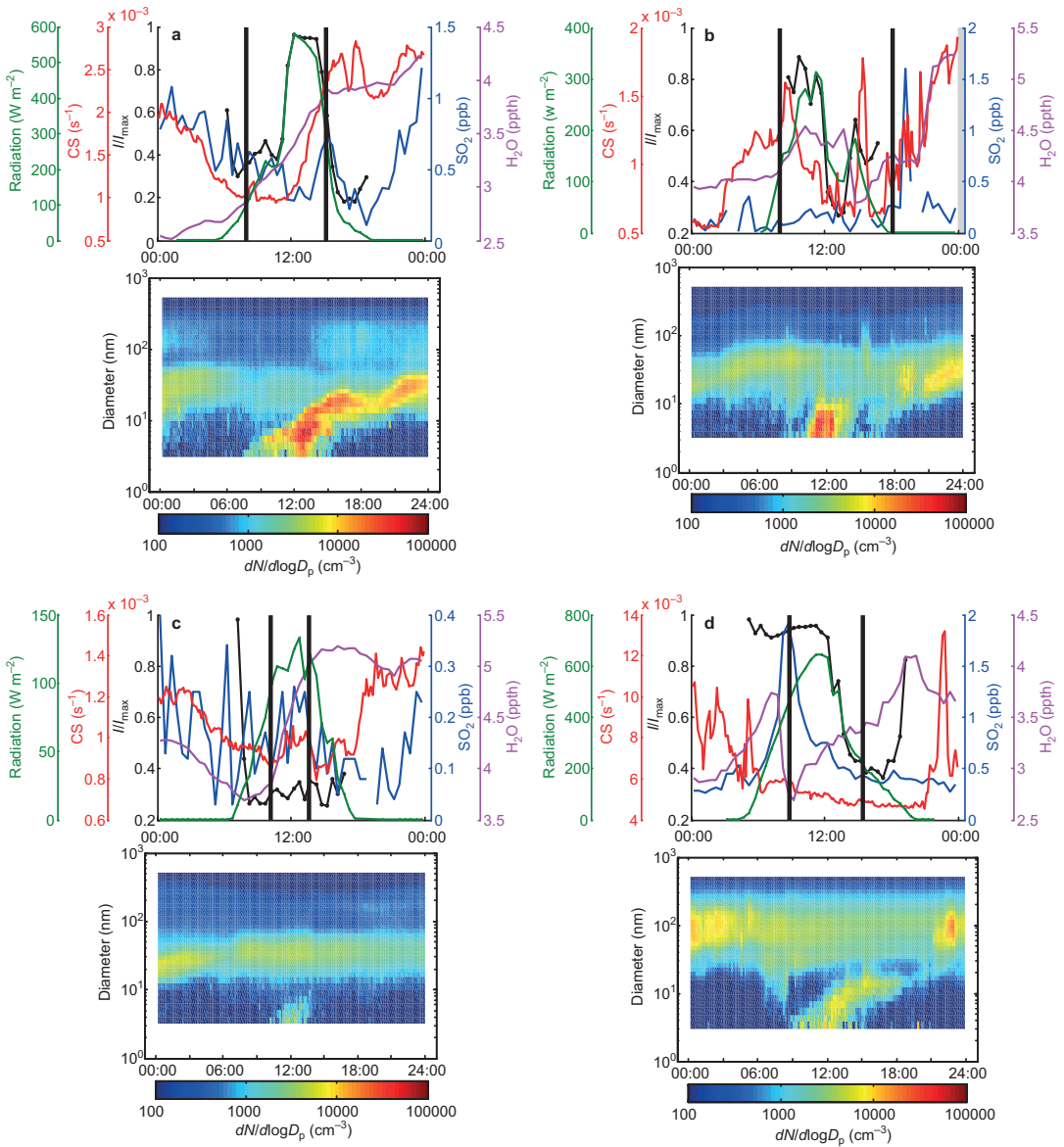


Fig. 8. Examples of Hyytiälä events of (a) type 1 (8 Apr. 2003), (b) type 2 (4 Oct. 2002), (c) type 3 (6 Oct. 2002) and (d) interrupted (26 Apr. 2004). Variations in environmental parameters *versus* the time of day are shown for CS (red curve), global radiation intensity (green curve), SO₂ concentration (blue curve) and H₂O (magenta curve). The black vertical bars in the plots show the period of NPF. The corresponding contour plots of particle number size distribution for each day are also presented.

Non-events associated with high values of III_{\max}

Investigation of non-events in which value of III_{\max} was above 0.8 (clear sky) for at least one hour revealed that very high values of CS (averages $5.3 \times 10^{-3} \text{ s}^{-1}$ and $19.2 \times 10^{-3} \text{ s}^{-1}$ in Hyytiälä

and SPC, respectively) prevented the occurrence of nucleation events. In addition, high concentrations of H₂O (average 11 ppb) and high temperatures (average 15 °C) in Hyytiälä might have contributed to the absence of NPF in clear-sky conditions.

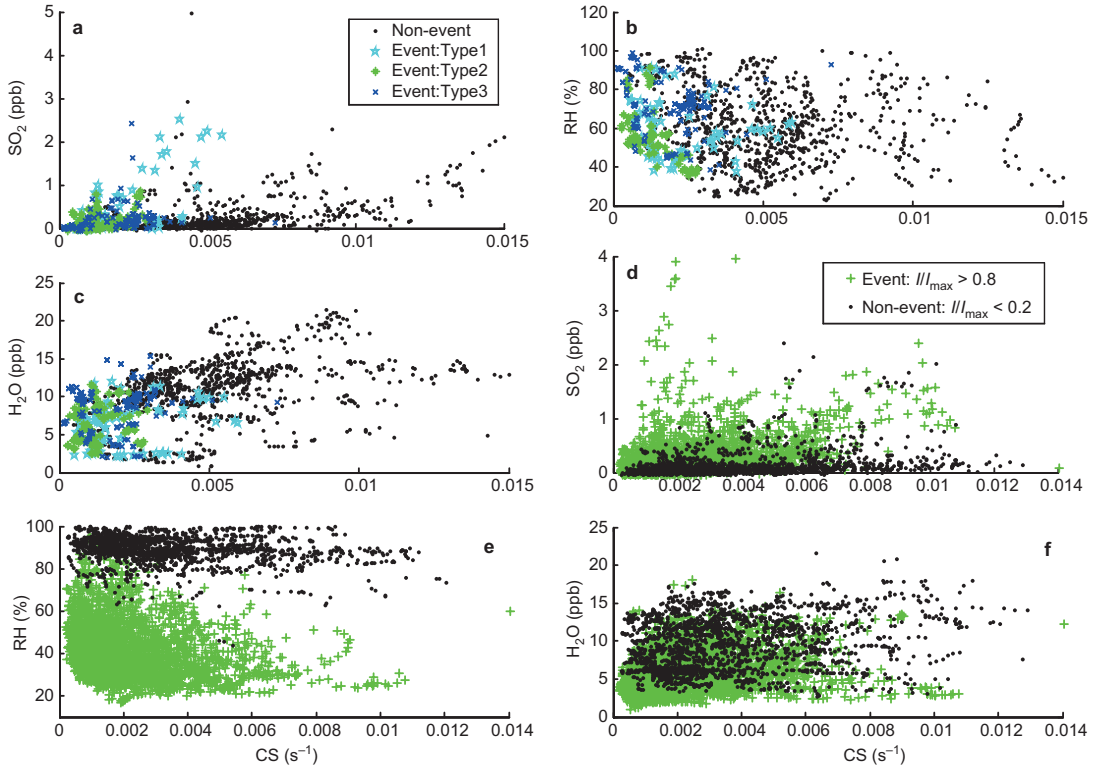


Fig. 9. SO₂ concentration, RH and H₂O concentration as a function of CS in Hyttiälä based on one hour-averaged data. Panels **a**, **b** and **c** show anomalous event days of type 1, 2 or 3 ($I/I_{max} < 0.5$) and anomalous non-event days ($I/I_{max} > 0.8$). Panels **d**, **f** and **e** show normal event days ($I/I_{max} > 0.8$) and normal non-event days ($I/I_{max} < 0.2$).

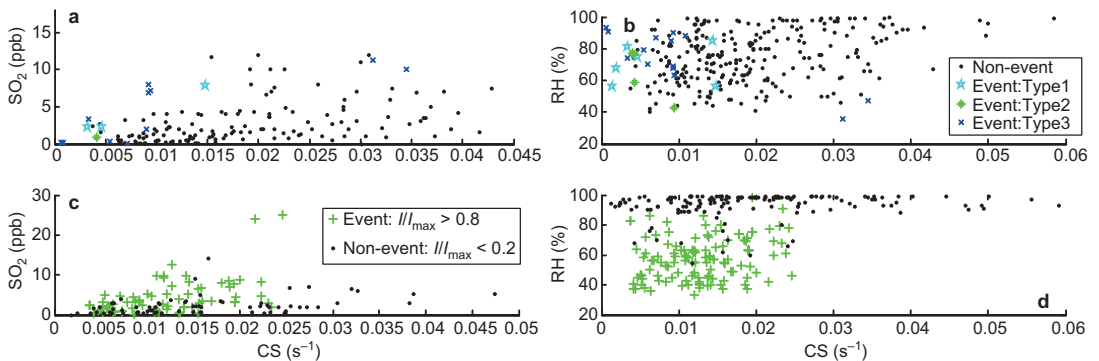


Fig. 10. SO₂ concentration and RH as a function of CS in SPC based on half and hour-averaged data. Panels **a** and **b** show anomalous event days of type 1, 2 or 3 ($I/I_{max} < 0.5$) and anomalous non-event days ($I/I_{max} > 0.8$). Panels **c** and **d** show normal event days ($I/I_{max} > 0.8$) and normal non-event days ($I/I_{max} < 0.2$).

Event interruption by increased cloudiness

During some event days with an initially clear sky, the appearance of clouds stopped nucleation and therefore the production of ultrafine parti-

cles. Our data included 56 and 10 such events in Hyttiälä and SPC, respectively; the NPF event on 26 Apr 2004 in Hyttiälä (Fig. 8d) being a good example. This event was associated with high values of CS (> 0.005 s⁻¹) during the whole

Table 2. The mean values of data points of different types of events and non-events presented in Fig. 9 for Hyytiälä.

	Non-event ($III_{\max} > 0.8$)	Non-event ($III_{\max} < 0.2$)	Event ($III_{\max} > 0.8$)	Event type 1 ($III_{\max} < 0.5$)	Event type 2 ($III_{\max} < 0.5$)	Event type 3 ($III_{\max} < 0.5$)	Interrupted events ($III_{\max} < 0.5$)
SO ₂ (ppb)	0.2714	0.1257	0.2390	0.4584	0.1535	0.2168	0.2360
CS (s ⁻¹)	0.0053	0.0036	0.0023	0.0019	0.0013	0.0018	0.0020
RH (%)	60	89	42	61	56	72	55
H ₂ O (ppth)	11	9	6	6	6	8	6

Table 3. The mean values of data points of different types of events and non-events presented in Fig. 10 for SPC.

SPC	Non-event ($III_{\max} > 0.8$)	Non-event ($III_{\max} < 0.2$)	Event ($III_{\max} > 0.8$)	Event type 1 ($III_{\max} < 0.5$)	Event type 2 ($III_{\max} < 0.5$)	Event type 3 ($III_{\max} < 0.5$)	Interrupted events ($III_{\max} < 0.5$)
SO ₂ (ppb)	2.8955	2.3184	4.2034	4.0964	0.8891	4.5042	4.6010
CS (s ⁻¹)	0.0192	0.0189	0.0129	0.0067	0.0055	0.0104	0.0130
RH (%)	74.9	93.2	58.2	70.1	63.8	74.3	58.2

period of NPF. However, the relatively high SO₂ concentration favored NPF despite the high value of CS until III_{\max} started to decrease, obviously slowing down the sulfuric acid production, which eventually caused the event to stop.

Summary and conclusions

In order to study the effects of clouds on NPF events in Hyytiälä and San Pietro Capofiume, we defined the relative radiation intensity, III_{\max} , as an indicator of cloudiness. The comparison between the event and non-event days showed that at both sites the fraction of event days generally increased with an increasing value of III_{\max} . At radiation levels below 50% of the corresponding clear-sky radiation ($III_{\max} < 0.5$) indicative of cloudy conditions, only a few NPF event days were found at both sites. Moreover, at radiation levels $0.5 < III_{\max} < 0.85$, the fraction of event days was much lower in SPC (22%) than in Hyytiälä (45%). This means that occurrence of a NPF event in SPC was highly likely only at close to clear-sky conditions.

We found that NPF can occur in cloudy conditions, provided that other environmental circumstances — in particular low condensation sink and high concentrations of SO₂ — are favorable. However, NPF events taking place at cloudy conditions tended to be rather weak, with

low number concentrations of freshly-formed particles. In some cases the appearance of clouds during NPF interrupted or decreased dramatically the production of 3 nm particles, while NPF could start again after the sky cleared. This feature is in agreement with the observation by Boy and Kulmala (2002). We conclude that, in agreement with Sogacheva *et al.* (2008), cloudiness can decrease the clarity of an NPF event and convert it to the non-quantifiable class.

We found a few non-event days under clear-sky conditions. Examination of the environmental data revealed that during those days, NPF had most probably been prevented by a high value of CS. Hyvönen *et al.* (2005) found that a criterion for separating event and non-event days that depends on both CS and RH can be created. Our analysis showed that the (apparent) RH-dependence of the event occurrence arises from “normal” conditions, i.e. clear-sky NPF events and cloudy non-events, whereas the CS dependence comes into play when the cloudy event days and clear-sky non-event days are examined. In future work, we aim to formulate a revised NPF event criterion with the help of the relative radiation intensity parameter.

Acknowledgments: This work was funded by the Cryosphere–Atmosphere Interactions in a Changing Arctic Climate project (CRAICC) by the ARPA supersite project, and by the Academy of Finland, the Center-of-Excellence program (project no. 1118615).

References

- Boy M. & Kulmala M. 2002. Nucleation events in the continental boundary layer: influence of physical and meteorological parameters. *Atmos. Chem. Phys.* 2: 1–16.
- Dal Maso M., Kulmala M., Riipinen I., Wagner R., Hussein T., Aalto P.P. & Lehtinen K.E.J. 2005. Formation and growth of fresh atmospheric aerosols: eight years of aerosol size distribution data from SMEAR II, Hyytiälä, Finland. *Boreal Env. Res.* 10: 323–336.
- Hamed A., Korhonen H., Sihto S.-L., Joutsensaari J., Järvinen H., Petäjä T., Arnold F., Nieminen T., Kulmala M., Smith J.N., Lehtinen K.E.J. & Laaksonen A. 2011. The role of relative humidity in continental new particle formation. *J. Geophys. Res.* 116, D03202, doi:10.1029/2010JD014186.
- Hamed A., Joutsensaari J., Mikkonen S., Sogacheva L., Dal Maso M., Kulmala M., Cavalli F., Fuzzi S., Facchini M.C., Decesari S., Mircea M., Lehtinen K.E.J. & Laaksonen A. 2007. Nucleation and growth of new particles in Po Valley, Italy. *Atmos. Chem. Phys.* 7: 355–376.
- Hyvönen S., Junninen H., Laakso L., Dal Maso M., Grönholm T., Bonn B., Keronen P., Aalto P., Hiltunen V., Pohja T., Launianen S., Hari P., Mannila H. & Kulmala M. 2005. A look at aerosol formation using data mining techniques. *Atmos. Chem. Phys.* 5: 3345–3356.
- Kerminen V.-M., Petäjä T., Manninen H.E., Paasonen P., Nieminen T., Sipilä M., Junninen H., Ehn M., Gagné S., Laakso L., Riipinen I., Vehkamäki H., Kurten T., Ortega I.K., Dal Maso M., Brus D., Hyvärinen A., Lihavainen H., Leppä J., Lehtinen K.E.J., Mirme A., Mirme S., Hörrak U., Berndt T., Stratmann F., Birmili W., Wiedensohler A., Metzger A., Dörmann J., Baltensperger U., Kiendler-Scharr A., Mentel T.F., Wildt J., Winkler P.M., Wagner P.E., Petzold A., Minikin A., Plass-Dülmer C., Pöschl U., Laaksonen A. & Kulmala M. 2010. Atmospheric nucleation: highlights of the EUCAARI project and future directions. *Atmos. Chem. Phys.* 10: 10829–10848.
- Kuang C., McMurry P.H., McCormick A.V. & Eisele F.L. 2008. Dependence of nucleation rates on sulfuric acid vapor concentration in diverse atmospheric locations. *J. Geophys. Res.* 113, D10209, doi:10.1029/2007JD009253.
- Kuang C., Riipinen I., Sihto S.-L., Kulmala M., McCormick A.V. & McMurry P.H. 2010. An improved criterion for new particle formation in diverse atmospheric environments. *Atmos. Chem. Phys.* 10: 8469–8480.
- Kulmala M., Petäjä T., Nieminen T., Sipilä M., Manninen H. E., Lehtipalo K., Dal Maso M., Aalto P.P., Junninen H., Paasonen P., Riipinen I., Lehtinen K.E.J., Laaksonen A. & Kerminen V.-M. 2012. Measurement of the nucleation of atmospheric aerosol particles. *Nature Protoc.* 7: 1651–1667.
- Kulmala M. & Kerminen V.-M. 2008. On the formation and growth of atmospheric nanoparticles. *Atmos. Res.* 90: 132–150.
- Kulmala M., Vehkamäki H., Petäjä T., Dal Maso M., Lauri A., Kerminen V.-M., Birmili W. & McMurry P. 2004. Formation and growth rates of ultrafine atmospheric particles: a review of observations. *J. Aerosol Sci.* 35: 143–176.
- Kulmala M., Lehtinen K.E.J. & Laaksonen A. 2006. Cluster activation theory as an explanation of the linear dependence between formation rate of 3nm particles and sulphuric acid concentration. *Atmos. Chem. Phys.* 6: 787–793.
- Kulmala M., Hämeri K., Aalto P.P., Mäkelä J.M., Pirjola L., Nilsson E.D., Buzorius G., Rannik Ü., Maso M. D., Seidl W., Hoffman T., Janson R., Hansson H.-C., Viisanen Y., Laaksonen A. & O’Dowd C.D. 2001. Overview of the international project on biogenic aerosol formation in the boreal forest (BIOFOR). *Tellus* 53B: 324–343.
- Laaksonen A., Kulmala M., Berndt T., Stratmann F., Mikkonen S., Ruuskanen A., Lehtinen K.E.J., Dal Maso M., Aalto P., Petäjä T., Riipinen I., Sihto S.-L., Janson R., Arnold F., Hanke M., Ücker J., Umann B., Sellegri K., O’Dowd C.D. & Viisanen Y. 2008. SO₂ oxidation products other than H₂SO₄ as a trigger of new particle formation — Part 2: Comparison of ambient and laboratory measurements, and atmospheric implications. *Atmos. Chem. Phys.* 8: 7255–7264.
- Mikkonen S., Romakkaniemi S., Smith J.N., Korhonen H., Petäjä T., Plass-Duelmer C., Boy M., McMurry P.H., Lehtinen K.E.J., Joutsensaari J., Hamed A., Mauldin R.L.III, Birmili W., Spindler G., Arnold F., Kulmala M. & Laaksonen A. 2011. A statistical proxy for sulphuric acid concentration. *Atmos. Chem. Phys.* 11: 11319–11334.
- Metzger A., Verheggen B., Dörmann J., Duplissy J., Prevot A. S.H., Weingartner E., Riipinen I., Kulmala M., Spracklen D.V., Carslaw K.S. & Baltensperger U. 2010. Evidence for the role of organics in aerosol particle formation under atmospheric conditions. *Proc. Natl. Acad. Sci. USA* 107: 6646–6651.
- Pirjola L. 1999. Effects of the increased UV radiation and biogenic VOC emissions on ultrafine sulphate aerosol formation. *J. Aerosol Sci.* 30: 355–367.
- Sihto S.-L., Kulmala M., Kerminen V.-M., Dal Maso M., Petäjä T., Riipinen I., Korhonen H., Arnold F., Janson R., Boy M., Laaksonen A. & Lehtinen K.E.J. 2006. Atmospheric sulphuric acid and aerosol formation: implications from atmospheric measurements for nucleation and early growth mechanisms. *Atmos. Chem. Phys.* 6: 4079–4091.
- Sipilä M., Berndt T., Petäjä T., Brus D., Vanhanen J., Stratmann F., Patokoski J., Mauldin R.L.III, Hyvärinen A.-P., Lihavainen H. & Kulmala M. 2010. The role of sulfuric acid in atmospheric nucleation. *Science* 327: 1243–1246.
- Sogacheva L., Saukkonen L., Nilsson E.D., Dal Maso M., Schultz D.M., De Leeuw G. & Kulmala M. 2008. New aerosol particle formation in different synoptic situations at Hyytiälä, southern Finland. *Tellus* 60B: 485–494.
- Weber R.J., Marti J.J., McMurry P.H., Eisele F.L., Tanner D.J. & Jefferson A. 1997. Measurements of new particle formation and ultrafine particle growth rates at a clean continental site. *J. Geophys. Res.* 102: 4375–4385.
- Schiffer R.A. & Rossow W.B. 1983. The International Satellite Cloud Climatology Project (ISCCP): The first project of the World Climate Research Programme. *Bull. Amer. Meteor. Soc.* 64: 779–784.